

Shallow-acceptor, donor, free-exciton, and bound-exciton states in high-purity zinc telluride

H. Venghaus

Max-Planck-Institut für Festkörperforschung, Stuttgart, Federal Republic of Germany

P. J. Dean

Royal Signals and Radar Establishment, Great Malvern, Worcestershire, England

(Received 13 April 1979)

Photoluminescence was measured at 1.6 K on ZnTe crystals, both nonintentionally doped high-purity and lightly P- or As-doped samples. Luminescence was excited mostly with a tunable dye laser close to the band gap. Ground states of the shallow-acceptor bound excitons are identified and attributed to the various acceptors by means of excitation spectra taken on two-hole satellites of these bound-exciton lines. Excited bound-exciton states are also obtained from the excitation spectra. The coupling of the electron and holes in the bound-exciton states appears to be very different for the various acceptors even for almost identical exciton localization energy. The excitation spectra of these two-hole luminescence satellites also exhibit negative spectral features attributed to the free-exciton 1S, 2S, and 3S levels. We derive the free-exciton binding energy $E_{FE}(1S) = 13.2 \pm 0.3$ meV and the band-gap energy $E_g = 2.3941 \pm 0.0004$ eV. Excitation spectra were also taken on the donor-acceptor pair bands involving the Li, P, As, and the Cu acceptor. These excitation spectra yield *s* and *p* symmetric excited acceptor states and also excited donor levels. The latter yield 18.3 ± 0.3 meV binding energy of the predominant shallow donor. Higher excited *nS* states ($n \geq 4$) for the Cu, Li, Ag, and the still unidentified *k* acceptor are derived from two-hole series measured on unintentionally doped samples. Our results thus represent the most complete information available to date on excited shallow-acceptor states in ZnTe. The donor-acceptor pair excitation spectra contain features due to the creation of TO(Γ) and LO(Γ) phonons and also impurity-dependent lattice vibrations. Two-electron satellite lines are observed for resonant excitation at the shallow-donor bound exciton. The results agree with those from the excitation spectra taken on the various donor-acceptor pair bands.

I. INTRODUCTION

ZnTe is a II-VI compound semiconductor with zinc-blende structure and a direct energy gap E_g close to 2.39 eV.¹ This energy corresponds to the green region of the spectrum and would be favorable for application as a visible-light emitting diode. However, ZnTe devices have not yet achieved commercial status, since it has not been possible to obtain *n*-ZnTe at moderate doping levels, but only for very high Al concentrations such as $2 \times 10^{20}/\text{cm}^3$ (Ref. 2). ZnTe lightly doped with impurities expected to introduce donors (Al for example) should be investigated to establish the reason for this behavior. However, before this can be done successfully the properties of typical acceptors must be known as well as possible. This will be the main subject of the present paper, extending, refining, and in certain instances correcting our earlier work on this subject.³ Some information on shallow donors will also be presented.

Similar to other direct-gap semiconductors, high-purity ZnTe exhibits a large amount of structure in its "edge luminescence" (cf. Fig. 1), corresponding to the radiative recombination of free and shallow-impurity bound excitons (BE), LO and TO replicas of these lines, two-hole transitions (radiative decay of acceptor bound excitons

leaving the remaining hole in an excited state), and also donor-acceptor-pair (DAP) transitions, if the donor concentration is sufficient. Free-electron to bound-acceptor-hole luminescence is favored other than at the lowest temperatures. About 10 different acceptors have been observed in our ZnTe samples, some of them identified as simple substitutional acceptors, others still unidentified or interpreted tentatively.^{3,4} Most of the acceptor bound excitons fall very close to each other (cf. Fig. 2). The question of which two-hole line and which acceptor bound-exciton ground state is related to the same acceptor is answered in Sec. III on the basis of excitation spectra (ES) of the different two-hole lines (i.e., scanning the excitation energy up to E_g while the detector is kept fixed at the energy of each two-hole transition in turn). Further these ES yield information about energy transfer between different impurity BE levels and also reveal excited BE states in general difficult to observe in low temperature ($\lesssim 4$ K) luminescence due to thermalization, but clearly seen in absorption.³

Excitation spectra of DAP luminescence are presented in Sec. IV. Excited donor and acceptor states are observed, although the energies of the latter are already above the donor ionization continuum. Moreover, the reduced (axial) symmetry allows us to study transitions to excited *p*- as well

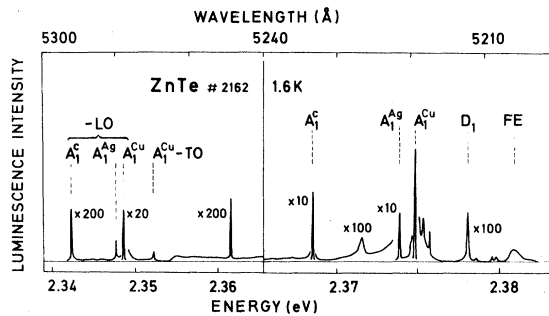


FIG. 1. Luminescence spectrum of an unintentionally doped high-purity sample for above band-gap excitation. Structures are due to radiative decay of free-exciton (FE), shallow-donor bound exciton (D_1), and acceptor bound excitons A_1^n ($n=Ag, Cu, c$). The low-energy region exhibits phonon replicas of the A_1^n transitions.

as s -symmetric states, in contrast to ordinary luminescence, where two-hole satellites corresponding to transitions to acceptor S -states strongly predominate. Experiments on samples having different impurity concentrations N_p show that excitation spectroscopy on DAP bands in ZnTe gives distinctive results for $10^{15}/\text{cm}^3 \leq N_p \leq 10^{17}/\text{cm}^3$. Excited states are determined by this technique for the Li, P, As, and Cu acceptors.

Excited donor states via two-electron transitions are not observed for above band-gap excitation, since acceptor bound-exciton transitions and the corresponding satellites are strongly predominant in p -type material. However, donor two-electron transitions can be observed for selective excitation at the donor bound exciton, and experimental results of this kind are presented in Sec. V.

II. EXPERIMENTAL

The experiments were performed on ZnTe crystals grown by a modified Bridgman technique in a carbon-lined quartz ampoule under Te-rich conditions at 1100°C .⁵ Most of the crystals used were not intentionally doped and had impurity concentrations $N_A - N_D \approx 10^{15}/\text{cm}^3$ according to electrical (Hall) measurements. Some samples were As or P doped with acceptor concentrations in the 10^{16} – $10^{17}/\text{cm}^3$ range.

For the photoluminescence measurements the crystals were freely suspended in liquid He pumped below the λ point. The luminescence was excited either with the $4765\text{-}\text{\AA}$ line of an Ar^+ laser, or alternatively with a tunable dye laser using a Coumarin 7 dye. Energy resolution of the dye laser was better than 0.1 meV . Signals were detected with a photomultiplier tube and a multi-channel analyzer system.

Crystals were thinned to $\sim 50\ \mu\text{m}$ for optical

transmission and certain excitation spectra by polishing first with carborundum, then with Br-methanol of increasing dilution. The final surface was of good optical quality and adequately damage-free.

III. EXCITATION SPECTRA OF TWO-HOLE LINES

A near band-gap luminescence spectrum of a not intentionally doped high-purity ZnTe sample is shown in Fig. 1. The spectrum exhibits free-exciton (FE), shallow-donor bound-exciton (D_1), and acceptor bound-exciton (A_1^n) luminescence, where n ($n=Ag, Cu, k, \dots$) refers to the different acceptors. Letters a, b, c, \dots were originally chosen arbitrarily to distinguish the different acceptors. The letters are now partially replaced by chemical symbols, where an acceptor could be identified as the corresponding atom acting as a substitutional impurity. Phonon replicas (TO, LO) of the various acceptor BE occur at appropriately lower transition energies. Two-hole transitions produce satellites at still lower energies. Bound-exciton and $2S$ two-hole satellite lines for the various shallow and moderately deep acceptors are compiled in Fig. 2. Two-hole lines are labeled A_m^n in the following for an acceptor of species n excited into the state m as A_1^n decays radiatively. A_1^n will be referred to as principal bound exciton (PBE).

In general, only two-hole lines related to acceptor $1S$ - $2S$ transitions are observed, however, in particularly pure samples whole series of excited acceptor states can be seen. Examples of two-hole series for the Cu and the Li acceptor were already shown in Refs. 3 and 4. (Cu is la-

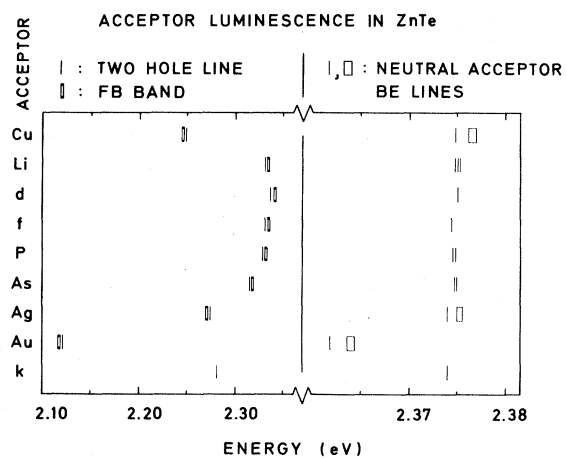


FIG. 2. A schematic diagram showing to the left the FB bands and two-hole PBE satellites and to the right the PBE lines for the indicated acceptors in ZnTe, both shallow and moderately deep. Broad acceptor BE structure is lifetime broadened.

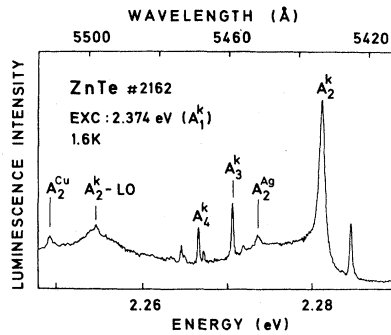


FIG. 3. Two-hole satellite series of the unidentified k acceptor observed for resonant excitation at the k -acceptor PBE A_1^k .

beled “ a -acceptor” in Refs. 3 and 4.) A two-hole series related to the k acceptor is shown in Fig. 3.

A. Cu-acceptor bound exciton

Excitation spectra of A_2^{Cu} are shown in Fig. 4. The spectra were taken on two different 0.6-mm thick crystals and on a 50- μm thick sample. An absorption spectrum of the latter is also included in Fig. 4. The apparent differences in the excitation spectra of the same two-hole line demonstrate that structures in these ES are not necessarily directly related to the luminescence line whose intensity is monitored, but positive as well as negative spectral features (peaks, dips) may in general be due to many other processes.

The identity of the 148-meV acceptor (labeled

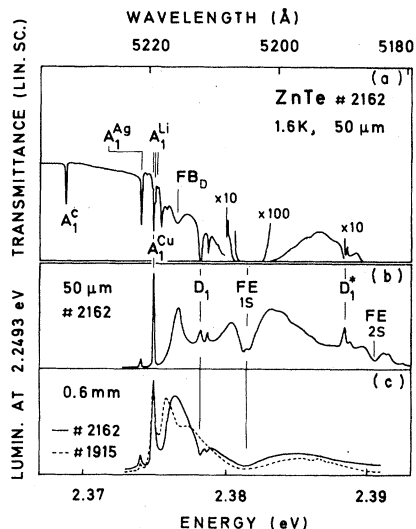


FIG. 4. (a) Transmittance spectrum of near band-gap region of 50- μm thick high-purity sample. The various structures identified are discussed in the text. (b) Excitation spectrum of A_2^{Cu} satellite line taken on the sample yielding the transmittance spectrum (a). (c) Excitation spectra of A_2^{Cu} satellite line taken on two different high-purity samples of 0.6-mm thickness, sample no. 1915 having extremely low donor concentration.

“ a -acceptor” before) has been established only recently as Cu_{Zn} ,⁶ and not V_{Zn} or a $V_{\text{Zn}}-D$ complex as frequently speculated heretofore.³ The Cu acceptor often defines the Fermi level in undoped refined ZnTe.

The strong and narrow excitation peak at 2.3749 eV occurs identically in all spectra and is attributed to the ground state of the Cu-acceptor bound exciton A_1^{Cu} . It coincides with the predominant luminescence line generally observed for above band-gap excitation in high-purity samples.

The dip at ~ 2.381 eV, attributed to the free exciton, is another structure which appears in a similar way in all spectra, while the shallow-donor bound exciton D_1 gives rise to a peak in excitation spectra measured on the 50- μm sample and produces a dip in thick crystals [cf. Figs. 4(b) and 4(c)].

Whether a feature in the excitation spectra of a given luminescence component will appear as a peak or a dip depends on the relationship of the crystal thickness and the absorption length for light of photon energy coincident with and immediately adjacent to the resonance under consideration. For example, the donor bound exciton D_1 appears as a well-defined dip in two-hole excitation spectra for crystals whose thickness is sufficient that all the light is absorbed in the vicinity of the D_1 line, probably mainly by acoustical phonon-assisted creation of neutral acceptor BE. In practice this applies for crystals of thickness $\gg 100$ μm at neutral acceptor concentrations typical for our undoped ZnTe, $3\text{--}5 \times 10^{15}/\text{cm}^3$. By contrast, D_1 appears as a peak in two-hole excitation spectra for crystals significantly transparent near D_1 such as the 50- μm thick crystal [cf. Fig. 4(b)], where $N_A - N_D$ is only $8\text{--}9 \times 10^{14}/\text{cm}^3$. Then absorption into D_1 is important for initial energy trapping in the crystal. Subsequent energy transfer between neutral acceptors by tunneling is probably responsible for the excitation of A_2^{Cu} (or in general A_2^a) luminescence from D_1 absorption. The most likely intersite energy-transfer mechanism involves tunneling to an excited state of the energy-receiving BE. This process will be most probable when the energy distributions of the receiving BE excited state and of the ground state of the donating BE overlap appreciably. We shall see that this condition holds for the A_1^{Cu} and D_1 bound excitons, since the sharply defined ground state D_1 overlaps the high-energy wing of the broad BE excited state A_1^{Cu} , described below.

Free-exciton absorption remains sufficiently intense near the resonance at 2.381 eV that this excitation process produces a dip even in 50- μm thick samples. Nonradiative surface recombination is likely to control the form of the excitation

spectrum close to the center of the free-exciton resonance.

A second component of the neutral donor BE is clearly evident in all these spectra 0.5 meV above D_1 (cf. Figs. 1, 4, and 7). It probably represents a higher angular momentum state of this BE complex, as recently discussed for InP,⁷ although no detailed study has yet been made for ZnTe.

Excitation spectra [Figs. 4(b) and 7, see below], like the absorption spectra of thin samples [Fig. 4(a)], also frequently exhibit impurity-related structure in the energy gap between the minima due to creation of the $N=1$ and $N=2$ states of the free exciton, discussed in Sec. III E. (Principal quantum numbers are designated by N to avoid confusion with n used in A_m^n to characterize two-hole lines.) Components D_1^* in Fig. 4 are attributed to donor BE associated with the $N=2$ FE on the evidence of spectral position and appropriately large diamagnetic shift rates.³ Similar structure has been seen in the spectra of crystals in which the acceptor BE are particularly prominent, for example, when A_1^{Cu} is enhanced by deliberate doping with Cu.⁶ The corresponding line $A_1^{\text{Cu}*}$ falls below D_1^* by 2.1₅ meV, rather less than the energy interval between A_1^{Cu} and D_1 , 3.2₅ meV. The oscillator strength of excitations to these states, particularly D_1^* , is expected to be greatly enhanced compared with even $N=1$ BE states because of the large orbital radii of $N=2$ BE states,⁸ substantiated by their large diamagnetic shift rates. This "giant oscillator strength" effect is also responsible for the strength of donor compared with acceptor $N=1$ BE states [Fig. 4(a)]. This is remarkable, because the concentration of the Cu acceptor is known to exceed that of the shallow donors in these p -type crystals.

Luminescence measurements at higher temperature (20.6 K) reveal a second component (labeled A_1^{Cu}) observed ~2.0 meV above A_1^{Cu} (Ref. 3). An energy of 2 meV was also measured for thermal activation in the intensity ratio $A_1^{\text{Cu}}/A_1^{\text{Cu}}$ (Ref. 9). However, owing to intensity arguments the broad absorption structure at 2.3768 eV cannot simply be interpreted as A_1^{Cu} . Magnetoluminescence experiments³ suggest A_1^{Cu} to be a $J=\frac{1}{2}$ state, and even if the absorption structure at 2.3768 eV is attributed to the unresolved $J=\frac{3}{2}, \frac{5}{2}$ levels, the intensity is too large compared to that of the A_1^{Cu} line to be consistent with this interpretation. A similar conclusion is obtained even if the BE splittings are predominantly caused by hole-hole coupling¹⁰ rather than the combination of hole-hole and electron-hole coupling as suggested initially.³ According to the energy position and the line shape we interpret the majority of the absorption structure at 2.3768 eV as (D^0, h) , i.e., neutral-donor-

free hole transitions. The FE binding energy of 13.2 meV [cf. Sec. III E, Eq. (3.1)] and 18.3-meV donor binding energy [cf. Sec. IV A 1, Eq. (4.1)] yield an expected energy separation of 5.1 meV between the (D^0, h) and FE structures, in good agreement with direct observation. These considerations suggest that the broad peak observed in the ES at 2.3768 eV is substantially due to (D^0, h) , masking weaker structure due to BE excited states.

In samples having extremely low donor concentration (such as sample no. 1915, concluded from the absence of D_1 and DAP emission) the (D^0, h) contribution to the ES is expected to be small; the differences at 2.376–2.377 eV in the ES shown in Fig. 4(c) could be explained accordingly. Under these circumstances the broken line in Fig. 4(c) should give the best result for A_1^{Cu} . However, 0.9-meV energy separation between A_1^{Cu} and A_1^{Cu} so derived differs from the luminescence results mentioned above, and thus we cannot give a definite answer with respect to A_1^{Cu} in our excitation spectra at present. It is probably necessary to make a closer study of appropriately thin samples from crystal 1915.

B. Li-acceptor bound exciton

The two-hole satellites of the Li-acceptor BE all appear as doublets. This is shown in Fig. 2 of Ref. 4. The magnitude of the splitting is apparently independent of the final acceptor state involved in the transitions, since luminescence lines corresponding to the $NS_{3/2}$ acceptor levels for different values of N as well as the structure related to the $2P_{5/2}(\Gamma_8)$ state all exhibit the same energy separation of 0.22 meV. Thus the observed splitting of the Li-acceptor two-hole satellites suggests that the initial BE state consists of (at least) two components separated by 0.22 meV. It is reasonable to assume thermalization between these two states for above band-gap excitation, and then equal intensity of the luminescence lines of a given doublet observed at 1.6 K implies that the relative strengths of the two components are 1:4.9. The determination of the energies of these two initial BE states was the purpose of the excitation spectra measured and shown in Figs. 5(b)–(d).

Excitation spectra of both A_2^{Li} components exhibit *three* peaks in the BE region with the expected 0.22-meV energy separation between the two lowest-energy states. The relative intensity of the components changes with detector setting and indicates that thermalization between the BE sublevels is incomplete for resonant excitation in contrast to excitation at higher energies. The third highest-energy structure corresponds to a BE sub-

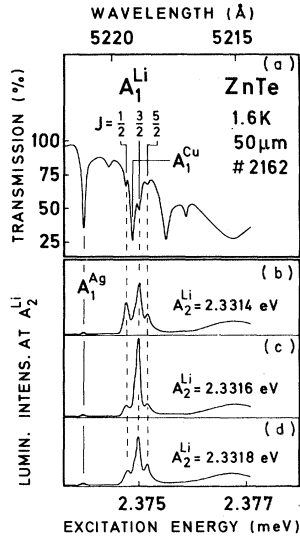


FIG. 5. (a) Small portion of transmittance spectrum as shown in Fig. 4(a), but in expanded energy scale. (b)–(d) Excitation spectra of A_2^{Li} satellite lines measured in PBE region. Spectra correspond to A_2^{Li} satellites of $J = \frac{1}{2}$ (b), $J = \frac{3}{2}$ (c), and $J = \frac{5}{2}$ (d)—subcomponents of Li-acceptor PBE (A_1^{Li}).

component which has no detectable two-hole satellite in ordinary luminescence at 1.6 K as a consequence of low oscillator strength and thermalization. The expected luminescence intensity of this component under full thermalization is only ~5% of the other components at 1.6 K. For the excitation spectrum shown in Fig. 5(d) ($A_2^{Li} = 2.3318$ eV) the detector was set to the energy expected for the two-hole satellite of this highest-energy BE sublevel, and in fact the corresponding structure becomes relatively pronounced in the ES.

The three Li-acceptor BE states are also observed in absorption on the same sample [Fig. 5(a)]. This spectrum indicates, that the lowest- and highest-BE component have approximately equal strength, while the central line is stronger. A precise determination of its relative intensity with respect to the other two states from absorption data is impaired by the A_1^{Cu} line falling close to the central A_1^{Li} state. Thus we take the result from luminescence for above band-gap excitation mentioned above and finally derive 1:4.9:1 relative intensities for the three A_1^{Li} BE sublevels.

This experimental result is in close agreement with the calculation of White *et al.*¹¹ For acceptor BE in direct-gap zinc-blende-type semiconductors and either $J = \frac{1}{2}, \frac{3}{2}, \frac{5}{2}$ or $J = \frac{5}{2}, \frac{3}{2}, \frac{1}{2}$ ordering of the BE substates, White predicted 1:4:1 relative strengths. Owing to the crystal field the $J = \frac{5}{2}$ level may be further split (or broadened). In the absorption spectra the highest-energy BE state is

definitely broader than the two others and thus we assume this to be the $J = \frac{5}{2}$ state. According to Ref. 11 this implies weak electron-hole interaction and attributes the observed splitting to the hole-hole interaction. However, the experimental intensity ratios are in rather poor agreement with the set predicted for the case of negligible electron-hole coupling 1:3:2 (Ref. 10). Our sequence of the BE levels is inverted from that observed for the shallowest acceptor BE in III-V semiconductors such as GaAs.¹²

C. Ag-acceptor bound exciton

Excitation spectra of the A_2^{Ag} luminescence line are shown in Fig. 6 for the 50- μ m and a 0.7-mm thick sample. The spectra exhibit dips related to FE absorption and donor BE related structure as discussed before. The strong and narrow line observed at 2.3740 eV represents the ground state of the Ag-acceptor BE. A second peak of similar integrated intensity at 1.3-meV higher energy is observed in the ES on the thick sample, while the corresponding structure appears an order of magnitude weaker in the ES on the 50- μ m sample. We attribute this peak to an excited state of the Ag-acceptor BE having much weaker oscillator strength than the ground state. The relative increase of the excited-state related structure in the thick sample can be explained in a simple way: Incident light having the energy of the BE *ground* state is absorbed by more than 50% in a 50- μ m thick layer for the given impurity concentration [cf. Figs. 4(a), 5(a)]. Consequently the luminescence intensity at A_2^{Ag} will increase at most by a factor of 2 even if the crystal is much thicker than 50 μ m. On the other hand, the absorption of photons having the energy of the BE *excited* state is low for a 50- μ m thick sample and the number of

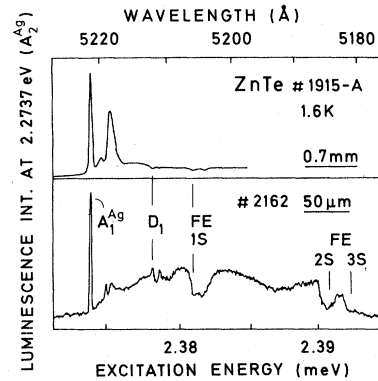


FIG. 6. Excitation spectra of Ag-acceptor two-hole satellite A_2^{Ag} taken on 0.7-mm and 50- μ m thick samples. FE 1S (2S, 3S) indicates position of transverse free-exciton ground state (2S-, 3S excited state).

photons absorbed into the Ag-acceptor excited BE state is almost proportional to the sample thickness even for 0.7 mm. Thus in the thick crystal the corresponding structure appears enhanced relative to the A_1^{Ag} line by an order of magnitude.

The Zeeman characteristics of A_1^{Ag} are very similar to those previously described for A_1^{Cu} (Ref. 3), interpreted in terms of a $J = \frac{1}{2}$ BE ground state. This fact and the behavior described here suggest a model similar to (Sn^0, X) in GaAs. The two-hole spins combine in a $J = 0$ state, while the single electron involved yields the total angular momentum $J = \frac{1}{2}$ of the BE ground state.^{13, 14}

The ES of A_2^{Ag} measured on the 50- μm sample exhibit a weak positive structure corresponding to A_1^{Li} ($J = \frac{3}{2}$) due to initial photocreation of A_1^{Li} and subsequent transfer of the excitation to A_1^{Ag} as discussed earlier. Absorption into A_1^{Cu} is much stronger than into A_1^{Li} as Figs. 4(a) and 5(a) demonstrate. The absence of a A_1^{Cu} -related peak in the ES taken on the 50- μm thick sample therefore indicates, that the energy transfer from A_1^{Cu} to A_1^{Ag} is much less efficient than that from A_1^{Li} ($J = \frac{3}{2}$) to A_1^{Ag} . The probable reason for this behavior follows from the description of the energy-transfer process given in Sec. IIIA. The spectral overlap between the $J = \frac{3}{2}$ component of A_1^{Li} and A_1^{Ag} is significantly greater than that for A_1^{Cu} and even more so for the $J = \frac{1}{2}$ component of A_1^{Li} (see Figs. 5 and 6). Once energy is captured into A_1^{Ag} by resonant tunneling, rapid internal relaxation to A_1^{Ag} with energy conservation by acoustic-phonon emission—proved by the lack of luminescence from A_1^{Ag} at 1.6 K—ensures that back transfer is very improbable.

D. k -acceptor bound exciton

We have recently recognized a further acceptor in some refined ZnTe crystals through careful examination of the two-hole satellites when this luminescence is selectively enhanced by photoexcitation into the appropriate parent BE absorption line (Fig. 3). For this unidentified k acceptor the ES reveals a single BE state at 2.3740 eV, i.e., degenerate with A_1^{Ag} (Fig. 7). The k - and Ag-acceptor BE coincide exactly, as nearly as can be determined, although the energies of the k and Ag acceptors are quite different (cf. Table II, below) and these BE are significantly shifted from the "main group" near 2.375 eV (Fig. 2). Thus this coincidence further dramatizes the futility of analyses which rely solely on the principal BE lines for spectroscopic identifications in ZnTe as well as many other direct-gap semiconductors, as has been clearly shown for GaAs.¹³

The structure observed at 2.375 eV is attributed

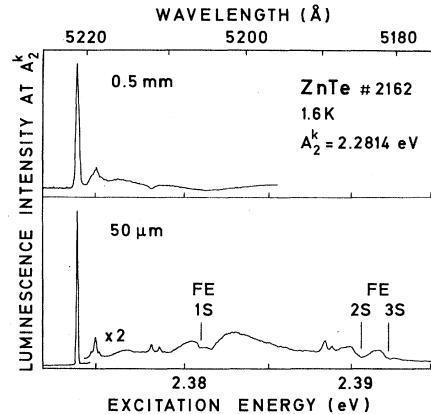


FIG. 7. Excitation spectra of unidentified k -acceptor two-hole satellite A_2^k taken on 0.5-mm and 50- μm thick samples of same crystal. FE 1S indicates transverse free-exciton ground-state energy. FE 2S, 3S label free-exciton excited states. Additional structures without label are easily identified by comparison with Fig. 4.

to A_1^{Li} . This is concluded from the relative intensity of the three subcomponents and from their energetic position, which is in exact coincidence with the three A_1^{Li} levels determined earlier (cf. Fig. 5).

The A_1^{Li} related structure preserves the shape of a peak in the ES of A_2^k measured on the 0.5-mm thick crystal in contrast to the behavior of the D_1 related structure, which appears as a dip in this case. This experimental observation suggests that the energy transfer from D_1 to A_2^k is much less effective than the transfer from A_1^{Li} to A_2^k , presumably for reasons similar to those just advanced to explain the effective transfer from A_1^{Li} to A_1^{Ag} . The ES obtained on the thick crystal exhibits less well-resolved structures compared to the 50- μm sample. This is interpreted as inhomogeneous broadening, since the experimental resolution was the same in both cases.

E. Free-exciton binding energy

The free-exciton related dips observed in the ES on the 50- μm thick sample can be used to derive the FE binding energy. Magnetorefectance measurements yield a broad structure ~ 8 meV above the FE attributed to the FE 2S state.¹⁵ Such a small 1S-2S energy separation $\Delta E(1S - 2S)$ is in disagreement with absorption data [cf. Fig. 4(a)]. However, optical absorption does not allow a precise determination of $\Delta E(1S - 2S)$, since we could not yet prepare samples sufficiently thin to reveal a narrow transition to the FE 1S state and clear resolution of the FE 2S from higher excited states. On the other hand, the ES provide precise experimental data. The FE 1S related structure exhibits

two relatively narrow dips attributed to the transverse and longitudinal exciton states, respectively. The energy separation of 0.7 meV between these two minima is in exact agreement with the longitudinal-transverse splitting obtained by line-shape analysis of normal incidence reflectance.¹⁵

We derive $\Delta E(1S-2S)=9.8_2$ meV and calculate according to Ref. 16 for $\mu=0.18$ (Ref. 17):

$$R_0 = 12.8 \pm 0.3 \text{ meV and } E_{FE}(1S) = 13.2 \pm 0.3 \text{ meV,} \quad (3.1)$$

where R_0 and $E_{FE}(1S)$ are the exciton Rydberg and ground-state binding energies, respectively. These results [Eq. (3.1)] are in very good agreement with the estimate obtained from the band parameters derived from our own optical measurements on free electrons and weakly bound holes in ZnTe.¹⁶ The 2S-3S energy separation calculated from Eq. (3.1), $\Delta E(2S-3S)_{\text{theor}} = 1.75$ meV is in perfect agreement with the experimental value $\Delta E(2S-3S)_{\text{exp}} = 1.7_2$ meV (Fig. 7). Using Eq. (3.1) and the transverse exciton energy E_{FE} (cf. Fig. 7) we derive

$$E_g = 2.3941 \pm 0.0004 \text{ eV} \quad (3.2)$$

as the band-gap energy in cubic ZnTe at 1.6 K.

IV. EXCITATION SPECTRA OF DONOR-ACCEPTOR-PAIR BANDS

A. ZnTe:Li

Excitation spectra measured on the DAP band at ~ 2.32 eV of a nominally undoped crystal are shown in Fig. 8. As will be discussed below, the residual shallow acceptor contributing most to this DAP band is Li. The two spectra given in Fig. 8 correspond to two different detector energy settings.

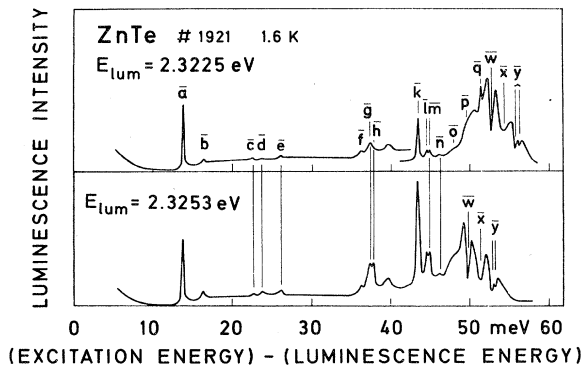


FIG. 8. Excitation spectra taken for two different detector settings on the DAP band of an unintentionally doped, highly compensated sample having $N_p \approx 10^{15}/\text{cm}^3$ impurity concentration. The various structures are discussed in Sec. IV A and identified in Table I.

TABLE I. Identification and excitation energies of structures observed in DAP excitation spectra of Figs. 8 and 9 (all energies in meV).

Line	Identification	Excitation energy	Binding energy
\bar{a}	donor 2S	13.7 ± 0.1	4.6
\bar{b}	donor 3S	16.2 ± 0.1	2.1
\bar{c}	TO(Γ)	22.5 ± 0.1	
\bar{d}	impurity-related phonon	23.6 ± 0.1	
\bar{e}	LO(Γ)	26.1 ± 0.1	
\bar{f}	second order phonons	36.0 ± 0.2	
\bar{g}	phonons	37.2 ± 0.1	
\bar{h}	Li- $2P_{3/2}$	37.8 ± 0.1	22.7
\bar{i}	P- $2P_{3/2}$	39.8 ± 0.1	23.7
\bar{k}	Li- $2S_{3/2}$	43.4 ± 0.1	17.1
\bar{l}	Li- $2P_{5/2}(\Gamma_8)$	44.5 ± 0.1	16.0
\bar{m}	P- $2S_{3/2}$	45.0 ± 0.1	18.5
\bar{n}	P- $2P_{5/2}(\Gamma_8)$	46.2 ± 0.1	17.3
\bar{p}	Li- $2P_{5/2}(\Gamma_7)$?	50.1 ± 0.3	10.4
	Li- $3S_{3/2}$	52.8 ± 0.3	7.7
\bar{w}	Cu-acceptor bound exciton A_1^{Cu}		
\bar{x}	neutral-donor-free hole (D^0, h) transition		
\bar{y}	shallow-donor bound-exciton states D_1, D_1'		

The structures observable in the ES can be classified into four different categories: (1) donor related structures, (2) structures associated with phonons, (3) structures which do *not* have constant energy separation to the detector, but which occur at fixed energies, and (4) structures corresponding to excited acceptor states.

The various lines and structures shown in Fig. 8 are identified in Table I. Entries in Table I and spectral features in Fig. 8 are correlated by the letters in order to avoid confusion with the letters labeling the unidentified acceptors. These two sets of letters have nothing to do with each other.

1. Shallow donor states

The lowest excitation peaks (\bar{a}, \bar{b} in Fig. 8) are attributed to donor excited states. This is in accordance with the fact that in a direct-gap semiconductor the donor is much shallower than the acceptor because of the low-electron effective mass m_e^* . A confirmation of this interpretation is provided by luminescence measurements with resonant excitation at the principal donor bound exciton D_1 as outlined in Sec. V A.

A simple hydrogenic model including polaron effects¹⁹ with a coupling constant $\alpha = 0.282$ yields for the donor 1S and 2S states the binding energies $E_D(1S) = 1.045 R_0^D$ and $E_D(2S) = 0.282 R_0^D$, where R_0^D is the donor Rydberg energy. The coupling constant α was calculated using $m_e^* = 0.11m_0$,²⁰

$\hbar\omega(\text{LO}) = 26.1$ meV (Ref. 3 and Table I), $\epsilon_0 = 9.3$ [see below, Eq. (4.3)], and $\epsilon_\infty = 6.9$. We calculated ϵ_∞ from ϵ_0 applying the Lyddane-Sachs-Teller relation with $\hbar\omega(\text{TO}) = 22.5$ meV (cf. Table I). If central cell corrections are neglected, the observed energy separation $E_D(1S) - E_D(2S)$ yields

$$R_0^D = 17.5 \pm 0.3 \text{ meV and } E_D(1S) = 18.3 \pm 0.3 \text{ meV} \quad (4.1)$$

for the shallow donor Rydberg and ionization energies, respectively. If $\epsilon_0 = 9.67$ (Ref. 1) and $\epsilon_\infty = 7.28$ (Ref. 21) are used to derive the polaron coupling constant α , we obtain $\alpha = 0.257$ and values for the donor Rydberg R_0^D and ionization energy $E_D(1S)$, differing less than 0.1 meV from the results given in Eq. (4.1).

For the energy separation between the donor 2S and 3S states we measure

$$E_D(2S) - E_D(3S) = 2.53 \pm 0.03 \text{ meV}. \quad (4.2)$$

This result [Eq. (4.2)] corresponds to $E_D(1S) = 18.2 \pm 0.3$ meV, i.e., the same donor binding energy as derived from the donor 1S–2S state energy separation.

This result is interesting for the following reason: 18.3 meV is relatively close to the TO phonon energy (cf. Table I) and according to Reference 22, $\epsilon(\hbar\omega = 18 \text{ meV}) \approx 10$, i.e., significantly larger than the static dielectric constant $\epsilon_0 \approx 8.3$ given in Ref. 22. If the donor 1S level is screened by an effective dielectric constant which is enhanced compared to the static value, the result would be a nonhydrogenic series for the donor 1S, 2S, 3S, ... levels. This is not observed, but the donor 1S, 2S, 3S states apparently all experience the same screening. The assumption that an enhanced screening of the donor 1S level by a larger effective dielectric constant might just be compensated by central-cell effects is rejected, since the central-cell corrections required are too large (~6 meV).

The effective (static) dielectric constant corresponding to the observed donor level separations is

$$\epsilon_0 = 9.3 \pm 0.2. \quad (4.3)$$

Finally, the donor ionization energy $E_D(1S)$ derived here is in agreement with the results obtained in Refs. 18 and 23.

2. Phonons

Structures \bar{c} – \bar{e} occurring in the 20–26 meV energy range are associated to the creation of single phonons. In particular, the 22.5- and 26.1-meV peaks (\bar{c} , \bar{e}) are attributed to the excitation of TO(Γ) and LO(Γ) phonons already known from the literature.²⁴

The nature of the 23.6-meV structure (\bar{d}) will be discussed in Sec. IV E. Two-phonon processes give rise to peaks in the 36–40 meV region of the ES. This is in agreement with second-order Raman measurements reported in Ref. 25.

3. Processes competing with DAP recombination

The highest-energy structures labeled \bar{w} , \bar{x} , and \bar{y} in Fig. 8 do not have constant energy separation with respect to the detected luminescence, but occur always at the same excitation energy. Comparison with luminescence and transmittance spectra demonstrates, that in this energy region the *minima* are the relevant structures, related to impurity bound-exciton states or to the free exciton (cf. Fig. 4). Bound-exciton recombination is much more efficient than energy transfer to the very distant DAP states whose recombination is selectively detected in these experiments, while the majority of the BE luminescence goes undetected. The principal reason for the extreme inefficiency of this energy-transfer process is the weakness of the DAP absorption isoenergetic with the BE or FE ground states. Also, distant DAP are inefficiently excited by FE photocreation. Minima associated with free-exciton states were already observed in the ES of two-hole satellites and attributed to surface effects (cf. Sec. III A).

4. Excited acceptor states, Li acceptor

The remaining structures of the ES shown in Fig. 8 correspond to acceptor states. The energy of the state associated with the predominant line \bar{k} is identical to the energy separation between the highest-energy two-hole satellite shown in Fig. 2 of Ref. 4 and the corresponding PBE. Accordingly, both lines are attributed to the same state and to the same acceptor, identified as Li from Raman measurements on heavily doped ZnTe:Li²⁶ and also from our own luminescence measurements on ZnTe Li-diffused in DRF-CENG, Grenoble. Comparison between the Li-related higher-energy two-hole satellites and the ES yields identification of the Li-3S_{3/2} level in the ES. It is observed only for still lower detector energies than those of Fig. 8. The energy obtained for the Li-3S_{3/2} state is different from the results reported in Ref. 26. Hattori *et al.*²⁶ derived only 5.8-meV energy separation between the Li-2S_{3/2} and Li-3S_{3/2} levels from Raman measurements in contrast to 9.4 meV determined here from the Li-PBE two-hole series. We regard the latter result as more reliable and conclude that the observed Raman line must be reinterpreted.

The intensity of line \bar{h} exhibits similar changes as the Li-2S_{3/2} structure when the detector energy

Excited phosphorus-acceptor states which are present in other samples like the unintentionally doped crystals are identified by comparison. In these cases the presence of minor relative concentrations of P may remain undisclosed by ordinary luminescence measurements (see below). On the other hand, the ES taken on the ZnTe:P samples reveal a considerable amount of Li in these P-doped crystals, particularly in the sample with $4 \times 10^{16}/\text{cm}^3$ impurity concentration [Fig. 9(b)]. This again could not be revealed by ordinary luminescence measurements, particularly because the BE lines became very diffuse for acceptor concentrations $>10^{16}/\text{cm}^3$ (Fig. 10, below). (3) The 1S - 2S state energy separation of the predominant shallow donor is the same within experimental error whether Li or P is the predominant shallow acceptor. The 2S donor level becomes very broad in the ES when the impurity concentration is increased from $4 \times 10^{16}/\text{cm}^3$ to $8 \times 10^{16}/\text{cm}^3$. This indicates that a well-defined 2S donor level separated from higher-excited donor states no longer exists. (4) The background underlying the excited acceptor state structures increases considerably with doping and limits the applicability of DAP excitation spectroscopy for the investigation of shallow acceptors in ZnTe to $\sim 10^{17}/\text{cm}^3$. This is not far below the solubility limit of substitutional incorporation without excessive precipitation for most acceptor species in ZnTe.

In addition to the ES as shown in Fig. 9 we also measured luminescence spectra for above band-gap excitation on the same samples (Fig. 10). In the case of the unintentionally doped crystal no. 1921 [Fig. 10(a)] a Li two-hole satellite line is observed in addition to Cu-acceptor BE related structure and broad features due to free-to-bound (FB) and DAP transitions. The presence of phos-

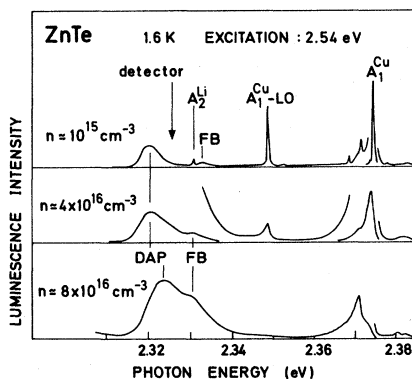


FIG. 10. Luminescence spectra taken for above band-gap excitation on the samples used for the ES shown in Fig. 9. The arrow marked "detector" indicates the detector energy for the ES shown in Fig. 9.

phorus cannot be deduced from this spectrum in contrast to the results provided by ES. The luminescence spectra of the P-doped samples [Figs. 10(b), (c)] are dominated by FB and DAP bands. The BE related structures become broader and shift to lower energies with increasing doping. This strong effect has been attributed to acceptor-acceptor interactions in the BE state.²⁷ Two-hole satellites are not observed at all and information concerning the identity of the acceptors involved in the observed spectra is completely lacking. Thus the advantages offered by ES compared to ordinary luminescence measurements are evident.

C. ZnTe:As

Excitation spectra measured on an As-doped sample are shown in Fig. 11. In addition to the donor and phonon related structures already discussed these spectra exhibit pronounced peaks due to creation of phonons and simultaneous donor excitation from the ground state to its 2S level. This higher-order process is particularly effective for the impurity-dependent phonon states (cf. Sec. IV E) but is hardly detectable when $\text{LO}(\Gamma)$ is involved.

The donor 2S - 3S energy separation measured on the As-DAP band is 13.8 meV, i.e., 0.1 meV larger than measured on the Li- or P-DAP bands. This is in contrast to the results of Nakashima *et al.*²³ who obtained 1.6 meV larger donor binding energy for ZnTe:As compared to ZnTe:Li, corresponding to 1.2-meV energy difference between the respective donor 1S and 2S levels. An explanation for this discrepancy exceeding our experimental error of 0.1 meV cannot be given at present.

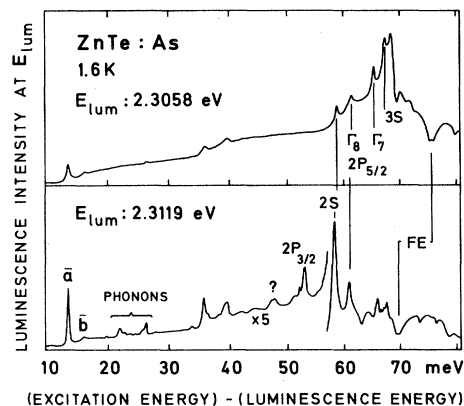


FIG. 11. Excitation spectra for two different detector energies within the As-DAP of an As-doped sample. Structure due to excited states of the As acceptor is labeled $2P_{3/2}$, 2S, etc. The phonon-dominated region of the ES is shown in an expanded energy scale in Fig. 12 and is discussed in Sec. IV E.

The observed excited states of the As acceptor are listed in Table II. The strongest acceptor related line occurring in the spectra is attributed to the As- $2S_{3/2}$ state. This assignment is in agreement with Raman measurements reported by Hattori *et al.*²⁶ and again with the two-hole satellites observed in our own conventional luminescence measurements on As-doped ZnTe. The $1S_{3/2} - 2S_{3/2}$ energy separation of the As acceptor increases continuously from 58.2 to 58.8 meV, as the detector is changed from 2.315 to 2.305 eV. Similar effects have already been observed for acceptor states in GaP (Ref. 28) and recently in ZnSe.²⁹ They are attributed to an interaction between the neutral donor and acceptor, which increases as the donor and acceptor become closer to each other.³⁰ Additional states are observed in the ES at 47.6 and 53.2 meV excitation energy. Both states have lower excitation, i.e., larger binding energy than the $2S_{3/2}$ state, although only one state ($2P_{3/2}$) is expected according to Ref. 16. By comparison with recent infrared absorption data³¹ the 53.2-meV peak is attributed to the As- $2P_{3/2}$ state, leaving the 47.6-meV structure unexplained.

Three more higher-excited states are also observed and included in Table II. The assignment of the last two levels is tentative, since the theoretical treatment given in Ref. 16 cannot be considered adequate for acceptors significantly deeper than an effective-mass acceptor.

D. Excited Cu-acceptor states

Excitation spectra taken on the Cu-DAP band exhibit 2S- and 3S-state related structure, and two additional peaks, which are attributed to the $2P_{3/2}$ and $2P_{5/2}$ (Γ_8) states. Assignment of the latter structures is in accordance with the considerations outlined in Ref. 18. Since the Cu-acceptor levels have already been discussed in Ref. 18, a detailed analysis will not be repeated here.

E. Impurity-dependent phonon states

Portions of excitation spectra which cover the energy range characterized by the creation of phonons are shown in Fig. 12. The spectra were measured on P- and As-doped samples. If Li is the predominant shallow acceptor, the phonon-related part of the ES is similar to that for ZnTe:P (cf. Figs. 8 and 12) and has therefore been omitted in Fig. 12. The structures labeled TO and LO are readily attributed to TO(Γ) and LO(Γ) optical phonons, emitted simultaneously with the creation of a neutral DAP in its ground state whose luminescence is then detected.

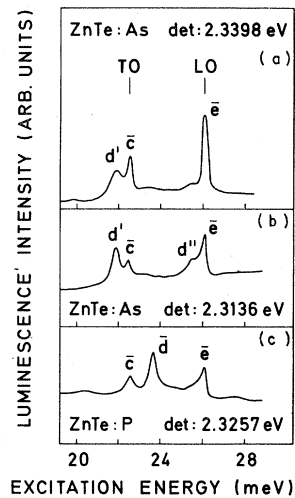


FIG. 12. Phonon-related part of excitation spectra for different doping and different detector energy. (a) ES on ZnTe:As, detector energy above As-DAP band. (b) ES on ZnTe:As, detector energy on As-DAP band. (c) ES on ZnTe:P, detector on P-DAP band.

The intensity ratio TO/LO is similar to that observed in selectively excited DAP luminescence as soon as the excitation energy falls significantly below the BE absorptions, and is much larger than observed in BE luminescence (Fig. 1). In this latter case coupling to LO(Γ) predominates because of the long-wavelength electric field related to the charge displacements associated with this vibrational mode.

We have previously identified the structure \bar{d} with an X optical phonon of the ZnTe lattice.³² However, the spectra in Fig. 12 indicate, that the position of this component is sensitive to the acceptor, and for As we observe instead of \bar{d} another line d' , falling below TO(Γ). In addition to the dependence of the energy of these components on the type of acceptor, Fig. 12 also shows a significant dependence of the relative intensity of phonon related structures on detector setting. The upper spectrum [Fig. 12(a)] was taken for a detector energy where DAP emission is very weak, in that case TO(Γ) and LO(Γ) are the most pronounced structures. The curve below [Fig. 12(b)] corresponds to a detector energy where DAP emission is strong, and in this case the relative intensity of TO(Γ) and LO(Γ) is considerably reduced.

Nakashima *et al.*³³ also observed the d' component in ZnTe:As and suggested that it might be a gap local mode. However, Scott *et al.*³⁴ report an increase in energy of this component by ~ 1 meV in a magnetic field of 14 T, while the energies of the TO(Γ) and LO(Γ) related lines are unaffected as expected. This result suggests that the \bar{d} and d' components are not primarily vibronic. The pos-

sibility that they are caused by the creation of an alternative type of bound phonon, whose frequency is determined by the local dielectric effect of the weakly bound hole on the neutral acceptor,³⁵ seems possible. However, the binding energy of such a phonon, measured by the energy displacement ΔE below the unperturbed $\hbar\omega(\text{LO})$, is expected to increase with decrease in acceptor ionization energy E_A , as long as $A_1^n - A_2^n$ remains larger than $\hbar\omega(\text{LO})$, in direct opposition to the behavior we find for \bar{d} and d' . By contrast, the observed decrease of ΔE in a large magnetic field is just as expected from the increase in energy $A_1^n - A_2^n$ this produces. It is perhaps possible that the large magnitude of ΔE for the As acceptor is related to a two-phonon interaction, since the relevant dominant excitation energy $E(\text{As}-1S_{3/2}) - E(\text{As}-2P_{3/2})$ only just exceeds $2\hbar\omega(\text{LO})$. This interpretation would imply a very strong hole-phonon interaction. We estimate the Fröhlich coupling constant $\alpha \sim 0.5$ for holes in ZnTe, consistent with the value ΔE we observed for the shallow acceptors Li and P, ~ 2.6 meV, much larger than for corresponding states in GaP, for example.³⁵ The additional component d'' about 0.7 meV below $\text{LO}(\Gamma)$ in Fig. 12 may represent a bound phonon of higher orbital angular momentum. Clear evidence for bound phonons has already been reported for neutral acceptors in ZnTe from the strong distortion they produce in the $\text{LO}(\Gamma)$ phonon replicas of the A_2^n two-hole transitions, particularly marked for the shallower acceptors such as Li, P, and As.³ It is interesting to note that the A_m^n two-hole satellites produce narrow and quite undistorted $\text{LO}(\Gamma)$ phonon replicas for transitions to higher excited states $m > 2$, even when the A_2^n replica is heavily broadened, shifted, and distorted as for relatively shallow acceptors like Li and P.³ This demonstrates very clearly the dominance of the $N=1 \rightarrow N=2$ electronic excitation in the hole-phonon interaction first recognized by Henry and Hopfield³⁶ in their discussion of donor BE in CdS.

V. SELECTIVELY EXCITED LUMINESCENCE AT SHALLOW-DONOR BOUND EXCITON

Resonant excitation at the shallow-donor bound exciton D_1 produces extra luminescence lines as shown in Fig. 13, attributed to two-electron transitions, i.e., recombination of the donor bound exciton D_1 and simultaneous excitation of the remaining donor electron. The donor $N=2$ state related luminescence structure is split into two components of comparable strength and an additional weaker component. We excited at the energy of an excited state of D_1 in Fig. 13(b) and observed two groups of luminescence lines at and slightly above the energy position labeled "2S". The high-

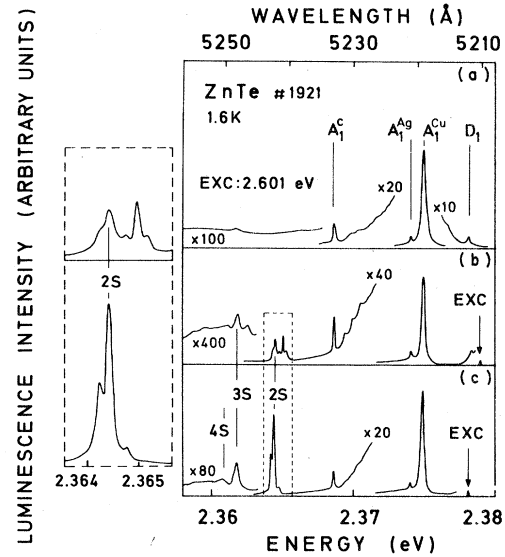


FIG. 13. Photoluminescence spectra of compensated high-purity sample for different excitation energies. (a) Excitation above bandgap; (b) excitation at donor BE excited state; (c) excitation at shallow-donor BE ground state D_1 . Donor two-electron transitions of spectra (b) and (c) are shown in expanded scale on the left-hand side. 3S and 4S indicate calculated donor 3S and 4S state.

er-energy group of lines is attributed to recombination from the excited state of D_1 and excitation of the remaining donor electron and the lower-energy luminescence lines are attributed to the corresponding process after relaxation to the D_1 ground state. The observation that the luminescence satellites related to the excited BE state similarly split as for excitation at the BE ground state rules out the possibility that the splitting as observed in Fig. 13(c) might be an artifact due to a corresponding energy difference between D_1 and the excitation energy.

The strongest two-hole luminescence line having 13.7-meV energy separation to the D_1 line is attributed to the $1S - 2S$ transition of the predominant shallow donor in agreement with the results of the DAP excitation spectra reported in Sec. IV. The second component, 13.9 meV below D_1 , can be interpreted in two different ways. One possibility is to attribute this structure to a different shallow donor. This would be in accordance with the results reported in Ref. 23. The observed donor $1S - 2S$ energy separation of 13.8 meV for the ZnTe:As sample (cf. Sec. IV C) may also be considered as a support for this interpretation. On the other hand, an energy difference between donor $2S$ and $2P$ states is expected due to different polaron enhancement of the binding energy.¹⁹ We calculated for $\alpha = 0.28$ (cf. Sec. IV A 1)

$E_D(2S) - E_D(2P) = 0.2$ meV energy difference between the donor $2S$ and $2P$ states in exact agreement with the experimentally observed energy difference between the two strong two-electron satellites. In addition to the calculated energy difference of 0.2 meV between the $2S$ and $2P$ donor states, there are two more arguments in favor of attributing the satellite falling 13.9 meV below D_1 to the donor $2P$ state. In ZnSe, $2S$ and $2P$ two-electron satellites are observed with approximately equal intensity and separated by 0.4 meV.³⁷ This larger energy separation compared to our result obtained on ZnTe is expected, since in ZnSe the shallow-donor binding energies are 25–28 meV (Ref. 37) and $\alpha = 0.45$. Thus the appearance of $2P$ satellites of intensity comparable to $2S$ related lines in ZnTe seems reasonable. A further argument supporting the assumption that $2S$ and $2P$ states of the same shallow donor are observed might be the following: We measured the same relative intensity for the 13.7- and 13.9-meV satellite lines in different samples. However, at this stage we cannot be certain that this is not fortuitous. The samples were not intentionally doped, were grown under similar conditions, and might have similar concentrations of the shallow donors, giving rise to the 13.7- and 13.9-meV satellite lines, according to our first alternative. A definite answer cannot be given on the basis of our experimental results concerning this particular point.

The much weaker structure having 13.4-meV energy separation to D_1 also cannot be interpreted definitely at present. However, our best suggestion is that this weak component involves a second (or third) donor species whose relative concentration is nearly constant in the few crystals in which we have been able to study these subcomponents with adequate precision.

VI. SUMMARY

Photoluminescence measurements at 1.6 K were performed on nonintentionally doped high-purity ZnTe crystals and also on lightly P- or As-doped samples. Shallow-acceptor bound-exciton states could be attributed to the various acceptors by means of excitation spectra taken on two-hole bound-exciton satellite luminescence lines. The localization energies of various acceptor bound excitons are almost the same for acceptor ionization energies E_A in the range $60 \text{ meV} < E_A < 150 \text{ meV}$. On the other hand, we observe large differences in the internal structure of the bound exciton states, i.e., different bound exciton subcomponents

due to different coupling of the electron and holes involved in the bound exciton states.

Excitation spectra of two-hole satellites also yield the free-exciton $1S$, $2S$, and $3S$ levels, since free-exciton absorption is a competing process to bound-exciton creation. This allows the experimental determination of the free-exciton binding energy $E_{FE}(1S) = 13.2 \pm 0.3$ meV and the band-gap energy $E_g = 2.3941 \pm 0.0004$ eV at 1.6 K.

Excitation spectra were also taken on the donor-acceptor pair bands involving the Li, P, As, and Cu acceptor. These excitation spectra yield s - and p -symmetric excited acceptor states, NS states in general up to $N=3$. Higher excited NS states for the Li, Cu, Ag, and the k acceptor are derived from two-hole series measured on unintentionally doped samples. The pair band excitation spectra further yield excited donor states giving the shallow-donor binding energy as 18.3 ± 0.3 meV. Finally, these spectra exhibit structure due to the creation of $TO(\Gamma)$ and $LO(\Gamma)$ phonons as well as impurity-dependent lattice vibrations.

Two-electron satellite lines are observed for resonant excitation at the shallow-donor bound exciton. The predominant line is in agreement with the donor $1S - 2S$ energy separation derived from the donor-acceptor-pair excitation spectra. A second satellite might either be due to a different shallow donor or to the donor $2P$ state, while a third weaker satellite probably involves a second (or third) donor species. The precise results of this optical study on high-quality ZnTe samples have given considerable additional confidence to the general, hitherto unexpected, result that all these dominant bound excitons in this semiconductor involve impurity-related acceptors.

ACKNOWLEDGMENTS

We are grateful to B. Schaub of Centre d'Etudes Nucléaires de Grenoble (CENG)–Laboratoire d'Electronique et de Technologie de l'Informatique (LETI) for the refined single crystals used in these experiments. We have also benefitted from Li, Ag, and Au diffusion-doped ZnTe crystals prepared by N. Magnea of CENG–Département de la Recherche Fondamentale (DRF), Grenoble. We are indebted to J. C. Pfister, N. Magnea, D. C. Herbert, and U. Rössler for numerous very informative and helpful discussions, to W. Senske and M. Sondergeld for help with the dye laser spectroscopy, and to W. Heinz for expert technical assistance.

- ¹B. Segall and D. T. F. Marple, in *Physics and Chemistry of II-VI Compounds*, edited by M. Aven and J. S. Prener (North-Holland, Amsterdam, 1967), p. 319.
- ²F. T. J. Smith, *Solid State Commun.* **9**, 957 (1971).
- ³P. J. Dean, H. Venghaus, J. C. Pfister, B. Schaub, and J. Marine, *J. Lumin.* **16**, 363 (1978).
- ⁴H. Venghaus, P. J. Dean, P. E. Simmonds, N. Magnea and J. C. Pfister, in *Proceedings of the 14th International Conference on the Physics of Semiconductors, Edinburgh, Gr. Britain, 1978*, edited by B. L. H. Wilson (Inst. Phys. Conf. Ser. No. 43, Institute of Physics, Bristol, 1979), p. 1279.
- ⁵B. Katircioglu, J. L. Pautrat, D. Bensahel, and N. Magnea, *Radiat. Eff.* **37**, 183 (1978).
- ⁶N. Magnea, D. Bensahel, J. L. Pautrat, K. Saminadayar, and J. C. Pfister, *Solid State Commun.* **30**, 259 (1979); D. Bensahel, N. Magnea, and M. Dupuy, *ibid.* **30**, 467 (1979); P. J. Dean, *J. Lumin.* **21**, 75 (1979).
- ⁷W. Rühle and W. Klingenstein, *Phys. Rev. B* **18**, 7011 (1978).
- ⁸E. I. Rashba and G. E. Gurgenshvili, *Fiz. Tverd. Tela* **4**, 1029 (1962) [*Sov. Phys. Solid State* **4**, 759 (1962)].
- ⁹N. Magnea, Ph.D. thesis, University of Grenoble, France, 1977 (unpublished).
- ¹⁰K. R. Elliott, G. C. Osbourn, D. L. Smith, and T. C. McGill, *Phys. Rev. B* **17**, 1808 (1978).
- ¹¹A. M. White, *J. Phys. C* **6**, 1971 (1973); A. M. White, P. J. Dean, and B. Day, *ibid.* **7**, 1400 (1974).
- ¹²A. M. White, I. Hinchliffe, P. J. Dean, and P. D. Greene, *Solid State Commun.* **10**, 497 (1972); U. Heim and P. Hiesinger, *Phys. Status Solidi B* **66**, 461 (1974), and references therein.
- ¹³D. J. Ashen, P. J. Dean, D. T. J. Hurle, J. B. Mullin, A. M. White, and P. D. Greene, *J. Phys. Chem. Solids* **36**, 1041 (1975).
- ¹⁴W. Schairer, D. Bimberg, W. Kottler, K. Cho, and Martin Schmidt, *Phys. Rev. B* **13**, 3452 (1976).
- ¹⁵H. Venghaus, P. E. Simmonds, J. Lagois, P. J. Dean, and D. Bimberg, *Solid State Commun.* **24**, 5 (1977).
- ¹⁶A. Baldereschi and N. O. Lipari, *Phys. Rev. B* **8**, 2697 (1973); **9**, 1525 (1974).
- ¹⁷H. Venghaus, B. Jusserand, and G. Behnke, *Solid State Commun.* **33**, 371 (1980). $\mu = 0.20$ according to R. A. Stradling, *Solid State Commun.* **6**, 665 (1968), would give $R_0 = 12.7$ meV, $E_{FE}(1S) = 13.2$ meV. $\mu = 0.22$ according to P. Lawaetz, *Phys. Rev. B* **4**, 3460 (1971), yields $R_0 = 12.6$ meV, $E_{FE}(1S) = 13.2$ meV, i.e., almost identical results.
- ¹⁸D. C. Herbert, P. J. Dean, H. Venghaus, and J. C. Pfister, *J. Phys. C* **11**, 3641 (1978).
- ¹⁹M. H. Engineer and N. Tzoar, *Phys. Rev. B* **5**, 3029 (1972); M. Engineer and N. Tzoar, *ibid.* **8**, 702 (1973).
- ²⁰P. J. Dean, H. Venghaus, and P. E. Simmonds, *Phys. Rev. B* **18**, 6813 (1978).
- ²¹D. T. F. Marple, *J. Appl. Phys.* **35**, 539 (1964).
- ²²A. Hadni, J. Claudel, and P. Strimer, *Phys. Status Solidi* **26**, 241 (1968).
- ²³S. Nakashima, T. Hattori, and Y. Yamaguchi, *Solid State Commun.* **25**, 137 (1978).
- ²⁴S. Narita, H. Harada, and K. Nagasaka, *J. Phys. Soc. Jpn.* **22**, 1176 (1967); J. L. LaCombe and J. C. Irwin, *Solid State Commun.* **8**, 1427 (1970); N. Vagelatos, D. Wehe, and J. S. King, *J. Chem. Phys.* **60**, 3613 (1974).
- ²⁵J. C. Irwin and J. LaCombe, *J. Appl. Phys.* **41**, 1444 (1970).
- ²⁶T. Hattori, S. Nakashima, and A. Mitsuishi, in *Proceedings of the 13th International Conference on the Physics of Semiconductors, Rome, 1976*, edited by F. G. Fumi (North-Holland, Amsterdam, 1976), p. 635.
- ²⁷P. J. Dean and A. M. White, *Solid State Electron.* **21**, 1351 (1978).
- ²⁸R. A. Street and W. Senske, *Phys. Rev. Lett.* **37**, 1292 (1976).
- ²⁹H. Tews and H. Venghaus, *Solid State Commun.* **30**, 219 (1979); H. Tews, H. Venghaus, and P. J. Dean, *Phys. Rev. B* **19**, 5178 (1979).
- ³⁰W. Senske, M. Sondergeld, and H. J. Queisser, *Phys. Status Solidi B* **89**, 467 (1978).
- ³¹S. Nakashima, T. Hattori, P. E. Simmonds, and E. Amzallag, *Phys. Rev. B* **19**, 3045 (1979).
- ³²H. Venghaus, P. J. Dean, P. E. Simmonds, and J. C. Pfister, *Z. Phys. B* **30**, 125 (1978).
- ³³S. Nakashima, H. Kojima, and T. Hattori, *Solid State Commun.* **17**, 689 (1975).
- ³⁴J. F. Scott, F. Habbal, J. H. Nicola, D. J. Toms, and S. Nakashima, *Phys. Rev. B* **19**, 3053 (1979).
- ³⁵P. J. Dean, D. D. Manchon, and J. J. Hopfield, *Phys. Rev. Lett.* **25**, 1027 (1970).
- ³⁶C. H. Henry and J. J. Hopfield, *Phys. Rev. B* **6**, 2233 (1972).
- ³⁷J. L. Merz, H. Kukimoto, K. Nassau, and J. W. Shiever, *Phys. Rev. B* **6**, 545 (1972).